# Dynamical hologram generation for high speed optical trapping of smart droplet microtools

**P. M. P. Lanigan,[1] I. Munro,[3] E. J. Grace,[3] D. R. Casey,[1] J. Phillips,[1] D. R. Klug,[1, 2] O. Ces,[1, 2] and M. A. A. Neil[1, 3, *]**

[1]*Single Cell Proteomics Group, Institute of Chemical Biology, Imperial College London, Exhibition Rd, London, SW7 2AZ, UK*
[2]*Department of Chemistry, Imperial College London, Exhibition Rd, London, SW7 2AZ, UK*
[3]*Department of Physics, Blackett Laboratory, Imperial College London, Prince Consort Rd, London, SW7 2AZ, UK*
[*]*mark.neil@imperial.ac.uk*

**Abstract:** This paper demonstrates spatially selective sampling of the plasma membrane by the implementation of time-multiplexed holographic optical tweezers for Smart Droplet Microtools (SDMs). High speed (>1000fps) dynamical hologram generation was computed on the graphics processing unit of a standard display card and controlled by a *user friendly* LabView interface. Time multiplexed binary holograms were displayed in real time and mirrored to a ferro-electric Spatial Light Modulator. SDMs were manufactured with both liquid cores (as previously described) and solid cores, which confer significant advantages in terms of stability, polydispersity and ease of use. These were coated with a number of detergents, the most successful based upon lipids doped with transfection reagents. In order to validate these, trapped SDMs were manoeuvred up to the plasma membrane of giant vesicles containing Nile Red and human biliary epithelial (BE) colon cancer cells with green fluorescent labelled protein (GFP)-labelled CAAX (a motif belonging to the Ras protein). Bright field and fluorescence images showed that successful trapping and manipulation of multiple SDMs in *x*, *y*, *z* was achieved with success rates of 30-50% and that subsequent membrane-SDM interactions led to the uptake of Nile Red or GFP-CAAX into the SDM.



**OSCIS codes:** (140.7010) Laser trapping; (230.6120) Spatial Light Modulators; (050.1970) Diffractive optics; (090.5694) Real-time holography; (170.0170) Medical optics and biotechnology; (180.0180) Microscopy.

## References and links

1. K. Svoboda, and S. M. Block, "Biological applications of optical forces," Annu Rev Biophys Biomol Struct **23**, 247-285 (1994).
2. A. Ashkin, J. M. Dziedzic, J. E. Bjorkholm, and S. Chu, "Observation of a single-beam gradient force optical trap for dielectric particles," Opt. Lett. **11**, 288-290 (1986).
3. E. Fällman, and O. Axner, "Design for fully steerable dual-trap optical tweezers," Appl. Opt. **36**, 2107-2113 (1997).
4. W. M. Lee, P. J. Reece, R. F. Marchington, N. K. Metzger, and K. Dholakia, "Construction and calibration of an optical trap on a fluorescence optical microscope," Nat. Protoc. **2**, 3226-3238 (2007).
5. K. Visscher, G. J. Brakenhoff, and J. J. Krol, "Micromanipulation by "multiple"optical traps created by a single fast scanning trap integrated with the bilateral confocal scanning laser microscope," Cytometry **14**, 105-114 (1993).
6. M. Reicherter, S. Zwick, T. Haist, C. Kohler, H. Tiziani, and W. Osten, "Fast digital hologram generation and adaptive force measurement in liquid-crystal-display-based holographic tweezers," Appl. Opt. **45**, 888-896 (2006).
7. J. W. Goodman, "Chapter 7," in *Introduction to Fourier Optics 3rd ed.*(Roberts & Co., 2004).

8. J. Leach, K. Wulff, G. Sinclair, P. Jordan, J. Courtial, L. Thomson, G. Gibson, K. Karunwi, J. Cooper, Z. J. Laczik, and M. Padgett, "Interactive approach to optical tweezers control," Appl. Opt. **45**, 897-903 (2006).
9. A. Lafong, W. J. Hossack, J. Arlt, T. J. Nowakowski, and N. D. Read, "Time-multiplexed Laguerre-Gaussian holographic optical tweezers for biological applications," Opt. Express **14**, 3065-3072 (2006).
10. T. Haist, M. Reicherter, M. Wu, and L. Seifert, "Using graphics boards to compute holograms," Comput. Sci. Eng. **8**, 8-13 (2006).
11. R. J. Rost, *OpenGL shading language* (Addison-Wesley, 2008).
12. National Instruments Corporation, "LabView 8.2.1.," (2007), http://www.ni.com/labview/.
13. R. H. Templer, and O. Ces, "New frontiers in single-cell analysis," J. Royal Soc. Interface **5**, S111-S112 (2008).
14. P. M. P. Lanigan, K. Chan, T. Ninkovic, R. H. Templer, P. M. W. French, A. J. de Mello, K. R. Willison, P. J. Parker, M. A. A. Neil, O. Ces, and D. R. Klug, "Spatially selective sampling of single cells using optically trapped fusogenic emulsion droplets: a new single-cell proteomic tool," J. Royal Soc. Interface **5**, S161-S168 (2008).
15. P. M. P. Lanigan, T. Ninkovic, K. Chan, A. J. de Mello, K. R. Willison, D. R. Klug, R. H. Templer, M. A. A. Neil, and O. Ces, "A microfluidic platform for probing single cell plasma membranes using optically trapped Smart Droplet Microtools (SDMs)," Lab on a Chip **9**, 1096-1101 (2009).
16. A. Salehi-Reyhani, J. Kaplinsky, E. Burgin, M. Novakova, A. J. deMello, R. H. Templer, P. Parker, M. A. A. Neil, O. Ces, P. French, K. R. Willison, and D. Klug, "A first step towards practical single cell proteomics: a microfluidic antibody capture chip with TIRF detection," Lab on a Chip **11**, 1256-1261 (2011).
17. NVidia, "GeForce 8600 " (2009), http://www.nvidia.com/object/geforce_8600.html.
18. Apple, "Working with Quartz Composer," (2009), http://developer.apple.com/graphicsimaging/quartz/quartzcomposer.html.
19. NVidia, "FX Composer 2.5," (2009), http://developer.nvidia.com/object/fx_composer_home.html.
20. University of Glasgow School of Physics and Astronomy, "Optical Tweezers Software," (2010), http://www.gla.ac.uk/schools/physics/research/groups/optics/research/opticaltweezers/software/.
21. B. R. Boruah, and M. A. A. Neil, "Susceptibility to and correction of azimuthal aberrations in singular light beams," Opt. Express **14**, 10377-10385 (2006).
22. M. A. A. Neil, M. J. Booth, and T. Wilson, "New modal wave-front sensor: a theoretical analysis," J. Opt. Soc. Am. A-Opt. Image Sci. Vis. **17**, 1098-1107 (2000).
23. B. Fowle, "Setting up OpenGL in an MFC control," (2006), http://www.codeguru.com.
24. M. Angelova, S. Soléau, P. Méléard, F. Faucon, and P. Bothorel, "Preparation of giant vesicles by external AC electric fields. Kinetics and applications," in *Trends in Colloid and Interface Science VI*, C. Helm, M. Lösche, and H. Möhwald, eds. (Springer Berlin / Heidelberg, 1992), pp. 127-131.
25. beepa, "Fraps real-time video capture and benchmarking," (2009), http://www.fraps.com.

## 1. Introduction

Optical tweezers are a popular technique in the biomedical sciences for reliably manipulating micron and sub micron sized particles, e.g. cells and beads [1]. Their popularity stems from the fact they provide a sterile, non-contact method, which if used at low powers have little or no detrimental side-effects to the specimen undergoing manipulation.

Originally a single beam gradient force optical trap was implemented by Ashkin in the 80s by using a single high numerical aperture (NA) objective lens [2]. In this case *x*, *y* steering is usually achieved by moving a microscope stage and *z* refocusing of the trap is possible by moving the objective or an external lens on the optical bench. Subsequently, multiple beam traps were introduced e.g. dual beam traps where a beamsplitter and mirrors in a 4-f arrangement allows for the steering of two independent optical traps [3, 4] in *x*, *y*, *z*. However, the use of 'bulk' optics becomes complicated when higher degrees of multiplexing are required and a power sharing approach is usually implemented either by a fast single scanning beam [5] with acousto-optic modulators or by holographic optical tweezers [6] using spatial light modulators (SLMs). This latter approach also allows the ability to refocus the individual beams to give full three-dimensional control of the multiple optical traps.

Holographic optical tweezers have been focussed on two different approaches. The first uses complex multi-output holograms to share the available power simultaneously amongst the required spot positions, and this approach must be followed when the spatial light modulator is slow, typically nematic liquid crystal SLMs [7]. There is a significant overhead however in the calculation of these complex spatially-multiplexed holograms, which demand both substantial software development and host computer time. A LabView based solution for generating these sort of holograms using various algorithms has been demonstrated by

Leach *et al* [8]. For faster SLM devices such as a ferro-electric liquid crystal SLM with ~10s μs switching times, a time multiplexed approach can be used where a sequence of much simpler holograms can be calculated and displayed in quick succession to scan the beam between the required spot positions. This approach is typified by the work of Lafong et. al. [9] who used OpenGL commands on the host PC to calculate holograms on a graphics card. However, their approach using geometrical drawing commands in OpenGL is still relatively complex and potentially inaccurate

In this contribution, we have used a ferro-electric liquid crystal on Silicon (FLCOS) SLM in a similar manner to Lafong *et al*. [9], where the 24 bit colour planes of the device display the required binary holograms for up to 24 independently steerable optical tweezer spots. However, instead of using convex polygons as described previously we have developed a method that uses the vertex and fragment shaders written in a simple C-like programming language running directly on the GPU. This takes advantage of the operational power of the GPU as demonstrated by Haist *et al*. who, using a Twisted-Nematic SLM (TN-SLM) for holographic tweezers and programming their GPU in Cg, managed to outperform a standard Pentium 4 (1-2GHz) CPU by at least ten to one [10]. The advantages of the GPU approach are that it calculates the hologram *in-situ* in video memory, thus avoiding the overhead of transferring the hologram data across busses in the computer, as well as making use of the multiple parallel processing cores typically available in the current generation of GPU chips. In our case we use the faster FLCOS-SLM displaying simpler binary holograms, which can be generated with as little as a single line of simple C-like code written in OpenGL Shading Language (GLSL) or similar low level graphics processing languages (Cg or HLSL) [11].

In our experiments, time-multiplexed optical tweezers that utilise 24-bit colour to encode the position of each optical trap require the calculation of each full holographic frame to be performed in ~700μs in order for the full 24-bit frame to be displayed at the 60Hz refresh rate of the graphics card and FLCOS SLM drive electronics. High-speed computation of holograms is essential for smooth trap manipulation as they are tracked across the field of view, including any necessary aberration corrections or the generation of helical phase or donut beams. Furthermore, to make the power of the GPU more accessible to non-specialists, we have developed an interface where variables to control the holograms can be passed into the GLSL text files from LabView 8.2.1. (National Instruments Corp), which has an easily accessible graphical user interface [12].

As an example of the operation of the system we demonstrate the use of optical trapping for single cell analysis. These methods are becoming crucial in understanding heterogeneity and cell-to-cell variations that cannot be detected from measuring averages in large populations [13]. To address this we have recently introduced a new proteomic tool that performs spatially selective sampling of the plasma membrane from single cells. This technology uses Smart Droplet Microtools (SDMs), which are optically trapped, emulsified oil droplets or beads with functionalised outer coatings. The coatings can be tailored for the specific interaction required with the cell and several types of these have been developed. SDMs coated with a 1,2-dioleoyl-*sn*-glycero-3-phosphocholine (DOPC) and 1,2-dioleoyl-*sn*-glycero-3-phosphoethanolamine (DOPE) mixture have fusogenic properties and following ~10 seconds contact with a target cell a membrane tether can be formed by steering the optically trapped SDM away from the cell-SDM docking site [14]. It has also been possible to remove membrane-anchored GFP from the cell's inner leaflet of the plasma membrane without forming a tether. In this case the SDMs were functionalised with an amphiphilic detergent molecule (Triton-X100), which is commonly used to solubilise cells. Furthermore, the introduction of a microfluidic device platform significantly aided in the storage and control of SDMs, allowing highly selective cell-SDM interactions to take place [15]. For the first time, we present SDMs with solid cores manufactured from 1μm silica spheres coated with a mixture of 9:1 DOPC and dimethylditetradecylammonium bromide (DMDTAB). These were prepared by the overnight shaking of silica spheres with an excess of small

unilamellar vesicles of the lipid mixture suspended in buffer, to form particles coated with one or more bilayers. The use of solid cores significantly increased trapping efficiencies and eliminated issues with SDM stability, buoyancy and polydispersity, while the addition of DMDTAB, a transfection reagent more commonly used in molecular biology protocols, presented CaaX-GFP sampling success rates as high as 50%.

We believe that for single cell manipulations and measurements to be used effectively, tools must be developed to allow precise, individual control of multiple traps. This is illustrated here by applying our dynamical holographic optical tweezer system to enable *x*, *y*, *z* control of SDMs to allow multiple, spatially selective sampling of giant vesicles and of the plasma membrane of biliary epithelial (BE) cells. This provides a robust method for sampling several distinct sites simultaneously on a cell surface in addition to making repeated measurements at the same site of interest. The development of such a flexible sampling platform may, when coupled to recent advances in single-molecule protein quantification [16], allow almost real-time read-out of the state of a cell membrane over its lifecycle. In this way, the behaviour of individual cells may be monitored and their individual responses to stimuli may be observed, revealing insights into their variation due to age, disease states or the administration of drugs or cell signalling agents.

## 2. Material and methods

### *2.2 Dynamical hologram generation*

The holograms were calculated on a NVidia GeForce 8600GT 512MB RAM GPU [17]. This processor has 32 processing pipelines that can run in parallel at clock speeds of up to 540MHz and with a total memory bandwidth of 80GB/sec. The output is displayed full-screen on a 1280 × 1024 pixel monitor, which is cloned to the FLCOS SLM (CRL-Opto SXGA-R-H1 1280 × 1024) used in the optical system for trapping. *Vertex* and *fragment* shaders running on the GPU were programmed in GLSL. Vertex and fragment shaders are key parts in the complex pipeline used to display graphics in highly realistic 3D games [11]. The basic idea of how shaders work is shown in the Fig. 1. In brief, an object e.g. triangle is outlined geometrically by a set of *user primitives* and these can then be transformed, e.g. stretched, translated and rotated by the vertex shader, in the case of 3D games in particular to allow rendering of the object from different viewpoints, but are also be used here to anamorphically scale the hologram as required. The job of the fragment shader is to then "shade" the object based on these transformed vertices on a pixel-by-pixel basis in respect of the output display device. This final operation is a highly parallelisable one and speed is achieved in modern graphics cards with a set of pipelined parallel processing cores; for details see [10, 11]. Using this approach the card used here can effectively independently calculate at 5.4 billion pixels/sec in parallel.

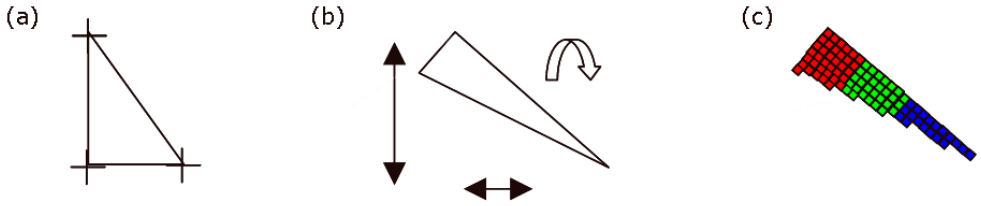


Fig 1. Basic idea behind GPU pipeline, (a) user primitives define an object to be manipulated and rendered, (b) the object is transformed by the vertex shader (c) the object is rendered by the fragment shader.

There are currently several available software suites that allow writing, debugging and optimisation of shaders. For example, Quartz Composer and FX-Composer are used for Macs and PC-based operating systems respectively, though not necessarily covering all GPUs.

There are also several different, yet similar shader languages that can be used, e.g. Cg and High Level Shader Language (HLSL) [18, 19]. It is also possible to write shaders without such tools due to their inherent simplicity and the limited nature of the programming language (see the "Orange book" [11]). To give the reader some idea of the simplicity of the code an extract of the key part is shown in Eq. (1).

```
{
    …
    colorsum=black;
    for(iter=0; iter<maxtraps; ++iter) {                    //loop over required traps
        if (sin(x*tiptilt[iter][0] + y*tiptilt[iter][1])<0) { //calculate binary hologram
            colorsum = colorsum + colourmap[iter];          //assign colour (on state)
        } else {
            colorsum = colorsum + OuterColor;               //assign black (off state)
        }
    }
    gl_FragColor = vec4(colorsum,1.0);      //24-bit pixel output value
}                                                                                    (1)
```

This simple 'for' loop, runs independently and once only at each pixel position in the hologram for each video frame that is output (at 60Hz in our case). The code binarises the desired tilted wavefront phase and then encodes the hologram pixel value with a colour (set of bit planes) stored in a look-up table (colourmap[iter]), for each trap of the total number of traps (maxtraps). The colour-coding look-up table is generated and indexed once by the LabView program and passed through to the shader along with the required spot positions as scaled values in the array tiptilt[][]. These two arrays are set globally and available to the fragment shader when it runs at each output pixel position; however the particular output pixel positions in the hologram, *x* and *y*, are interpolated by the graphics card using values from the vertex shader and passed to the fragment shader code individually at each pixel depending on the hologram pixel position being calculated. Thus each trap can be time-multiplexed into colour bit planes as has been previously been shown [9] with maxtraps sharing 24/maxtraps colour bit planes. The last line in this code sets the output pixel value of the pixel that is then sent to the display. In our case this is transmitted digitally to the SLM over a DVI-D cable link and the SLM drive circuitry then displays each of the 24 bit-planes in sequence for an equal length of time on the FLCOS device. With this approach the dwell time can be shared equally between 1, 2, 3, 4, 6, 8, 12 or 24 traps, or unequally shared between any number up to 24 traps. Aberration correction and defocus for individual traps are easily accommodated in the above code at the binarisation stage, and indeed are included in the full version of the shader code used by our LabView user interface.

*2.3 LabView user interface*

An important aspect of this research was to allow non-specialised users to utilise the operational power of the GPU for high speed holographic trapping. We therefore chose LabView 8.2.1 to be the front-end of the technology as this has a user friendly graphical interface and pre-coded virtual instruments that control peripheral devices such as cameras and motorised stages [12]. LabView is also a relatively high level language and is becoming more popular amongst scientists who have little or no knowledge of text based coding languages such as C. Indeed other LabView based spatially multiplexed holographic optical trapping software with GPU processing are available for download, for example from the University of Glasgow [20].

The designed interface displays controls for selecting the number of traps and for Zernike mode aberrations. It also features sliders for independent, high NA defocus for each trap and

topological charge setting for helical phase or donut beam generation. The hologram aspect ratio could be configured on the fly as well as controls to open and close the OpenGL hologram window. Aberration correction of anti-symmetric Zernike modes was achieved by viewing the quality of a reflected donut beam, which was imaged in reflection off of an IR mirror with a CCD [21]. For symmetrical aberrations e.g. spherical, a modal wavefront sensor as described by Neil at al. was implemented [22].

As described in the previous section, variables such as Zernike modes and high NA defocus etc. were passed into the GLSL *via* the 'call library function' node in LabView, which loaded the MFC -DLL Release version of the precompiled C++ code. In this case the call library function interface node was configured to use the recommended Standard API (Application Interface) convention. The DLL also contained functions to open and close the hologram; the former had additional code to display the hologram fullscreen on the hologram designated monitor. The DLL itself had 3 layers; a class to communicate with LabView; a class that contained OpenGL commands, which set-up the OpenGL window including the viewport, user primitives and reading shaders and the third class to create the OpenGl window in an MFC dialog box. Fortunately much of the OpenGL-MFC code is open source and there are several developer sites on the internet that are available to get an application started, a good example of which can be found in [23]. The vertex and fragment shaders were written in MS note pad and saved as rich text files, which were called by the OpenGL class. Variables passed in by LabView were passed to the shaders using OpenGL commands with ARB extensions as described in the Orange book [11].

As described the majority of variables were sent to the fragment shader of the GPU excluding the hologram's aspect ratio, which was sent to the vertex shader. This was used to correct for the elongated appearance of the hologram in the *x*-direction due to the larger number of pixels i.e. *x*/*y* pixel ratio = 1280/1024 = 1.25.

The LabView code itself consisted of two state machines in parallel that controlled the hologram generation and camera acquisition respectively. The latter saved images in .png format, movies in .avi format and displayed the trap position with a colour coded square onto the image window, see Fig. 2 for layout of LabView interface.

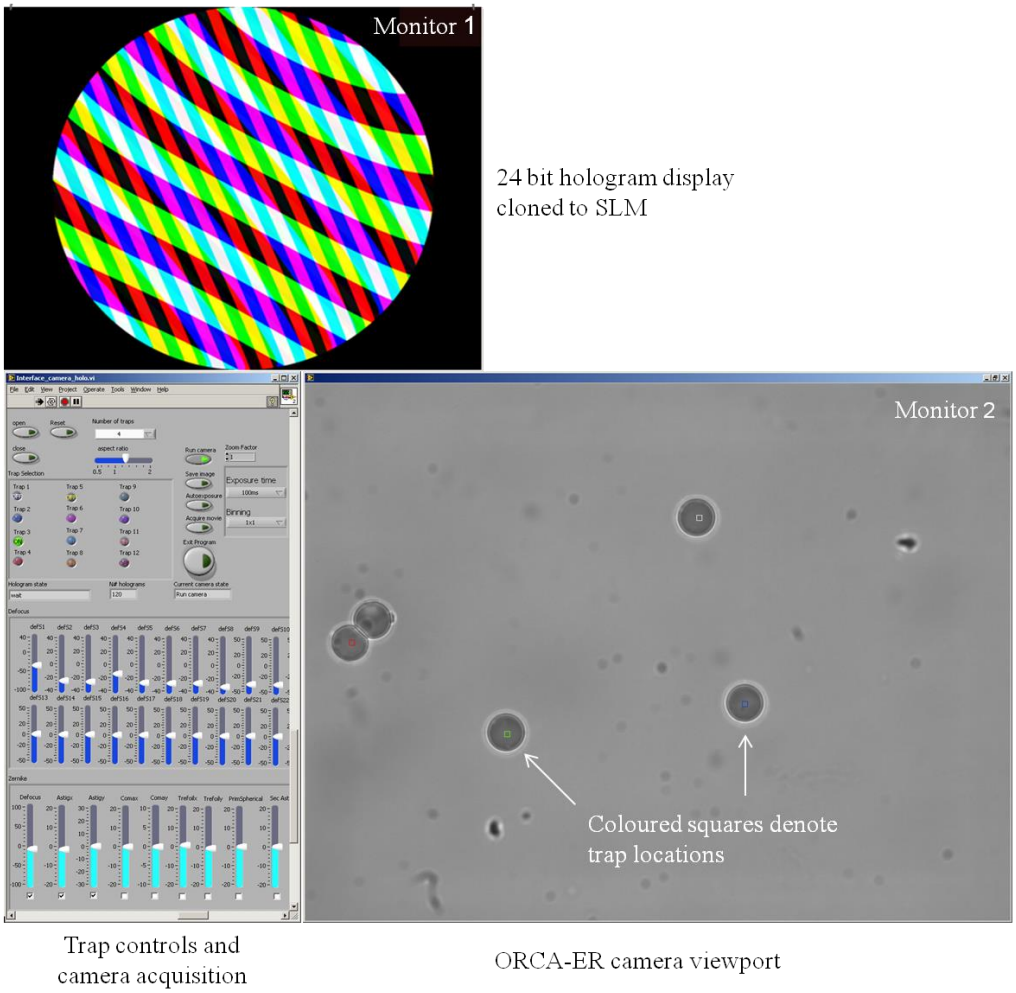


Fig. 2. Shows LabView user interface for dynamical hologram generation and trap manipulation. Two displays were used, monitor 1 (17-inch 1280×1024 pixels) for the OpenGL window for displaying the shaded 24 bit holograms and monitor 2 (24-inch 1920×1200 pixels) for the number of traps selection, defocus, aberration correction and camera acquisition controls.

*2.4 Optical trapping set-up*

The optical set-up was built around a Nikon TE2000-U inverted microscope fitted with a stage riser for the fitting of two stacked carousels. The upper carousel contained the Nikon cube with IR trapping dichroic (Chroma Corp) and was directly beneath the 60× 1.2NA water immersion objective used in all trapping experiments. Alignment of the set-up was made by using the transillumination light source used for bright-field and a phase contrast objective 10× or 20×. Two IR coated doublets (Linos photonics, QiOptic) were then used to form an image of the phase ring on the SLM. To accommodate the large size of the SLM (20mm square), the lenses were chosen to slightly reduce the image of the SLM at the pupil plane of the objective using two IR doublets f = 200mm and f = 160mm respectively (Linos Photonics, QiOptic). The laser used was a Ytterbium fibre laser with linear polarisation and at a wavelength of 1070nm. The fibre optic output of the laser was collimated to a large beam

diameter of 8mm, which was then expanded by a factor of 2.5 by another set of IR coated doublets, f = 40mm and f = 100mm respectively (Linos Photonics, QiOptic). Furthermore two half-wave plates were placed before and after the SLM and before a 25mm polarising beam-splitter (Edmund Optics), in order to dump the unwanted unmodulated beam into a purpose built commercial beam-dump (Thorlabs), (see Fig. 3 for a schematic of the optical system built). The optical throughput of the system measured at the pupil plane of the objective was ~10% with losses mainly due to the poor diffraction efficiency of the SLM in the IR.

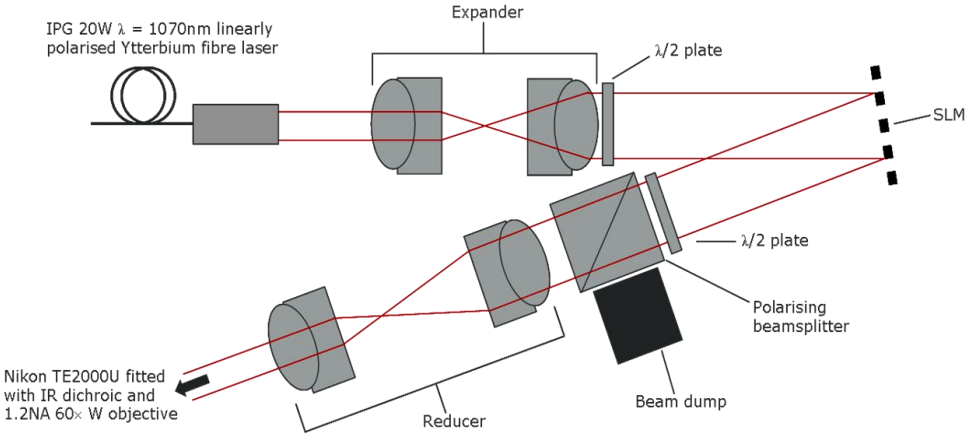


Fig 3. Showing optical trapping set-up, the IR laser source was expanded onto the SLM, which was then imaged onto the back aperture of the microscope objective lens. The half-wave plates and polarising beamsplitter selected out the phase modulated diffracted beam from the unmodulated dc component.

*2.5 SDM, cell and giant vesicle preparation*

Liquid core SDMs were prepared as previously reported from emulsions of heptanes or hexadecane stabilised in water by either Triton-X 100 a mixture of DOPE and DOPC [13, 14]. Solid cores were prepared using small unilamellar vesicles of 90% DOPC 10% dimethylditetradecylammonium bromide (DMDTAB), mol:mol. In brief, around 0.5mg of the mixture of lipids were co-dissolved in chloroform and then evaporated to dryness under a nitrogen stream. The resulting lipid film was re-suspended in 2ml Dulbecco's phosphor-buffered saline (PBS) and extruded ten times through 2 x 200nm polycarbonate membranes (Whatman, USA) in a Lipex high-pressure extruder (Northern Lipids, Canada).

0.5ml of the resulting suspension was mixed with 1µl of a suspension of 1µm silica spheres (5% by weight in water, Sigma-Aldrich, UK) in a 1.5ml Eppendorf vial and shaken overnight at approximately 450 rpm. The beads were then centrifuged to a pellet, the supernatant removed and the beads re-suspended in fresh PBS. This process was repeated to remove any excess lipid and once re-suspended in PBS were stored at 4ºC to await their use.

GFP-expressing human BE colon cancer cells were prepared as previously described elsewhere [14, 15], while giant unilamellar vesicles of DOPC containing 1% Nile Red dye were prepared by electroformation from indium tin oxide-coated glass [21]. The vesicles were grown in a 200mM sucrose solution, then diluted 99:1 with 200mM glucose solution in order that they sank, for ease of study.

## 3. Results

*3.0 GPU performance testing*

To gain insight into the operational power of the GPU in generating holograms on the fly, a commercial game profiling and benchmarking tool was used [25]. This tool auto-detects OpenGL windows and displays an on screen frame count.

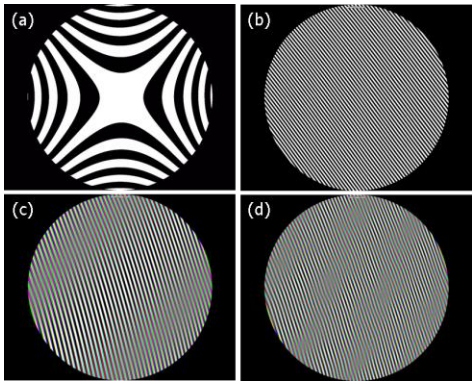


Fig. 4. Screen shots showing dynamical (a) aberrations (Media 1), (b) single spot scanning(Media 2), (c) 3 spot scanning (Media 3) and (d) one spot scanning from a 12 spot time-multiplexed hologram (Media 4).

1-24 bit time-multiplexed holograms were tested in turn and the on screen frame count was measured to be 60Hz, i.e. for 24 bit planes, 24×60 =1440 holograms/sec. Furthermore, this tool was used to record the OpenGL window as it is commonly used for video game trailers. Screen shots of dynamical hologram generation including aberration and spot scanning are shown in Fig. 4.

*3.1 Testing the system*

In order to test the hologram generation a preliminary optical set-up was used which directed a 2mW, 532nm, diode pumped solid state laser (DPSS) (Scitec Instruments) onto the SLM. The resulting diffraction pattern was then focussed by a lens into a fluorescence slide (Complementary fluorescently doped orange slide, Chroma Corp), which was in turn magnified a 100 times onto an ORCA-ER CCD (Hamamatsu) by a 10× microscope objective and eyepiece (Linos Photonics, QiOptic) respectively. Examples of $x$, $y$, $z$ manipulation, aberration correction and helical phase beams with increasing topological charge are shown in Fig. 5.

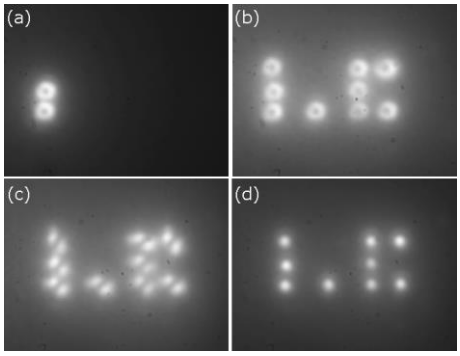


Fig. 5. Shows (a) *x, y*, manipulation of donut beams (Media 5), (b) independent *z* manipulation of donut beams (Media 6), (c) manual aberration correction (Media 7) and (d) donut beams with increasing topological charge (Media 8).

### *3.2 Cell-SDM trapping experiments*

The ability of the optical system to trap was tested with three forms of the lipid and detergent coated SDMs as shown in Fig. 6.

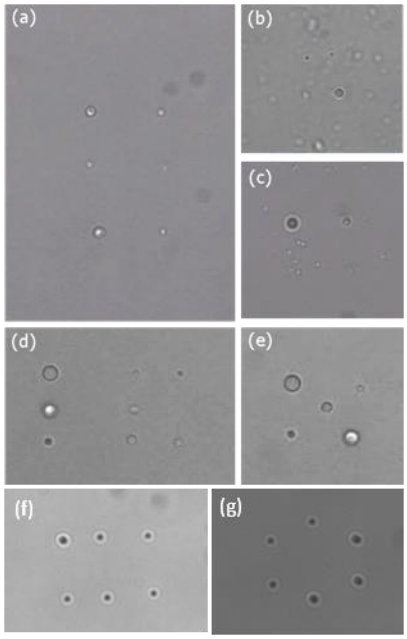


Fig. 6. Shows test trapping on (a-c) Triton –X100 (Media 9-11), (d,e) DOPE/DOPC coated fluid SDMs (Media 12, 13) and DOPC/DMDTAB-coated silica SDMs (Media 14-15): (a) *x, y* manipulation of 6 trapped SDMs, (b) stage scanning with 4 trapped SDMs, (c) *z* manipulation of 4 trapped SDMs, (d-e) *x, y* manipulation of 8 and 6 SDMs respectively, (f) stage scanning with 6 Si SDMs and (g) *x, y* manipulation of 6 Si SDMs.

It was found that the trapping set-up was not power limited and ~50mW per trap (measured at the back aperture of the microscope objective) was sufficient to trap all types of SDMs, although it was found that approximately 10-20% more power was required for Triton-X coated droplets which was likely to be due to the lower index of refraction of the heptane core.

The target system was loaded into a perfusion chamber on a microscope cover-slip, to minimise evaporation. 1µl SDM suspension was added and the mixture placed on the microscope stage. The point-and-click interface was then used to select multiple SDMs, which were then brought up sequentially to different sites of the membrane. After incubation times of 2 minutes, SDMs were removed from the cell and fluorescence microscopy used to visualise the uptake of the dye or EGFP-labelled CAAX. Fluorescence and bright-field images of exemplar multiply trapped SDM-cell interactions are shown in Fig. 7. Sampling rates varied between the different SDM formulations and target systems: typical rates for the silica-cores blobs were around 30% for EGFP uptake from cells and 50% for Nile Red from vesicles. Major causes of failure were the loss of the SDM either to permanent membrane adhesion or due to its displacement from the trap due to collision with floating debris.

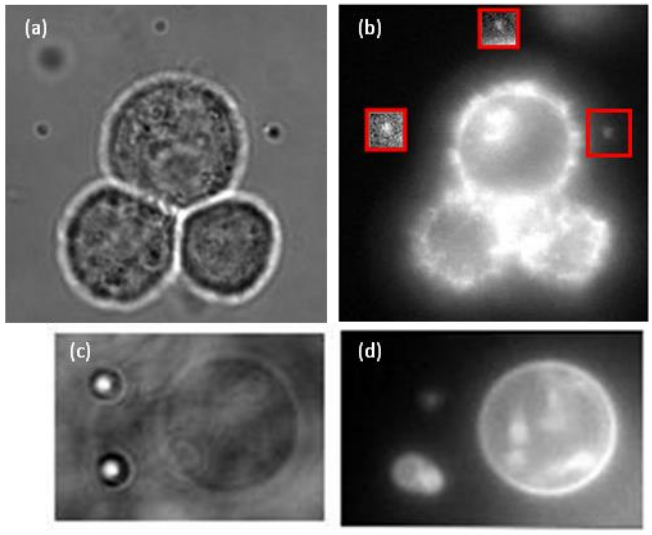


Fig. 7. Bright-field (a) and fluorescence (b) images showing SDM-cell interactions at multiple sites on BE-cell surface. Brightness of SDMs 1 and 2 has been increased for clarity; SDM 3 is clearly visible without amplification. This clearly demonstrates different levels of either protein expression or sampling efficiency across the surface of the cell membrane. Sampling was significantly simpler from giant vesicles, shown in bright-field (c) and fluorescence (d) channels.

## 4. Summary

We have successfully demonstrated spatially selective simultaneous chemical digestion at multiple sites on the plasma membrane of human BE colon cancer cells using the recently introduced SDMs. These digestions were non-destructive, and no obvious alterations in cell function or viability were observed during or after sampling. This technique offers the potential for multiple samplings of a cell or cells of interest at regular time-points throughout their life-cycle, revealing information that would otherwise be averaged out in traditional cell-lysate analyses.

This takes advantage of a holographic optical tweezer system that can control multiple SDMs in 3D ($x$, $y$, $z$) by time-multiplexing the 24 bit planes of a FLCOS SLM and displaying binary holograms. We have combined this with the operational power of the GPU programmed in GLSL, which can be controlled by a user friendly LabView interface *via* a MFC -DLL. We believe that this is a practical solution to generating dynamical holograms in real time that can be conveniently controlled by a non-specialist computer programmer. Furthermore, this retains the full utility and functionality of LabView e.g. the writing of

simple programs for instrument control, which is a popular language amongst scientists with little or no formal training in computer science.

**Acknowledgements**

We would like to thanks EPSRC for the award of grants EP/C54269X/1 and EP/I017887/1. Ed Grace is generously supported by a fellowship from the RAE/EPSRC.